Available online at www.sciencedirect.com

ScienceDirect

Journal of Ocean Engineering and Science 4 (2019) 263–275

www.elsevier.com/locate/joes

Original Article

# Investigations of Soret, Joule and Hall effects on MHD rotating mixed convective flow past an infinite vertical porous plate

M. Veera Krishna[a,*], B.V. Swarnalathamma[b], Ali J. Chamkha[c,d]

[a] *Department of Mathematics, Rayalaseema University, Kurnool, Andhra Pradesh 518007, India*

[b] *Department of Science and Humanities, Stanley College of Engineering & Technology for Women, Abids, Hyderabad, Telangana 500001, India*

[c] *Department of Mechanical Engineering, Prince Sultan Endowment for Energy and Environment, Prince Mohammad Bin Fahd University, Al-Khobar 31952, Saudi Arabia*

[d] *RAK Research and Innovation Center, American University of Ras Al Khaimah, 10021, United Arab Emirates*

Received 23 March 2019; received in revised form 10 May 2019; accepted 10 May 2019
Available online 16 May 2019

**Abstract**

We made an elaborate scrutiny on the Soret and Joule effects of MHD mixed convective flow of an incompressible and electrically conducting viscous fluid past an infinite vertical porous plate taking Hall effects into account. Perturbation technique is used to solve the non-dimensional equations. The effects of the various non-dimensional parameters on velocity, temperature and concentration within the boundary layer are examined. Besides that, computational deliberations or discussions are also undertaken on the effects of the pertinent or significant parameters on the skin-friction coefficient and rates of heat and mass transfer in terms of the Nusselt and Sherwood numbers respectively. The concentration distribution increases with increase in Soret effect and decrease with increase in chemical reaction parameter. An increase in Prandtl number results to decrease the temperature distribution. Both the primary and secondary velocity components and temperature increases with increasing heat source parameter. Skin friction coefficient decreases with an increase in permeability parameter, whereas it shows reverse effect for thermal and mass Grashof numbers. Nusselt number increases with an increase in Prandtl number. Sherwood number reduces with increasing Soret number.



*Keywords:* Hall effects; Soret number; Porous medium; Joules dissipation; Chemical reaction.

## 1. Introduction

Rapid efforts have been made to study the effects of various fields in porous media by both experimentally and theoretically. Flows through porous medium are of principal interest in the fields of agricultural engineering, underground water resources and seepage of water in river beds, filtration and purification processes in ocean engineering, petroleum technology to study the movement of natural gas, oil and water through the oil reservoirs. The way in which fluid flow through porous media is of great importance for the petroleum extraction processes. Most of the problems have considerable practical significance besides contributing more to the existing knowledge. Porous materials due to their inherent capability are widely used in Ocean engineering, Mechanical engineering, Medical appliances and Modern industrial fields.

The theory of rotating fluids (Greenspan [33]) is highly important because of its occurrence in various natural phenomena and technological situations which are directly governed by the action of Coriolis force. The broad areas of Oceanography, Meteorology, Limnology and Atmospheric Science all contain some important and essential features of rotating fluids. The fluid flow problems in rotating medium have drawn attention of many researchers who investigated hydrodynamic flow of a viscous and incompressible fluid in rotating medium considering different aspects of the problem. There has been considerable interest in the problems of hydromagnetic flow

* Corresponding author.
*E-mail addresses:* veerakrishna_maths@yahoo.com (M.V. Krishna), bareddy_swarna@yahoo.co.in (B.V. Swarnalathamma), achamkha@pmu.edu.sa (A.J. Chamkha).

https://doi.org/10.1016/j.joes.2019.05.002

**Nomenclature**

| | |
|---|---|
| $u$, $w$ | components of velocity in $x$ and $z$directions (m/s) |
| $g$ | acceleration due to gravity (m/s$^2$) |
| $T$ | dimensional temperature of the fluid (K) |
| $T_\infty$ | temperature far away from the plate (K) |
| $T_w$ | temperature near the plate (K) |
| $C$ | dimensional concentration of the fluid (Kgm$^{-3}$) |
| $C_w$ | concentration near the plate (Kgm$^{-3}$) |
| $C_\infty$ | concentration far away from the plate (Kgm$^{-3}$) |
| $k$ | permeability of porous medium (m$^2$) |
| $B_0$ | applied magnetic field (A/m) |
| $C_p$ | specific heat of the fluid at constant pressure (J Kg$^{-1}$ K) |
| $w_0$ | constant suction velocity (m/s) |
| $D$ | chemical molecular diffusivity (m$^2$/s) |
| $D_1$ | coefficient of thermal diffusivity (m$^2$/s) |
| $k_1$ | thermal conductivity of the fluid (w m$^{-1}$ k$^{-1}$) |
| $k_2$ | chemical reaction rate constant (mol L$^{-1}$ s) |
| $P_e$ | electron pressure (N m$^{-2}$) |
| $B$ | magnetic field vector (A/m) |
| $E$ | electric field (c) |
| $V$ | velocity vector (m/s) |
| $J$ | current density vector (A/m$^2$) |
| $Gr$ | thermal Grashof number |
| $Gm$ | mass Grashof number |
| $Pr$ | Prandtl number |
| $R$ | rotation parameter |
| $Sc$ | Schmidt number |
| $So$ | Soret number |
| $Ec$ | Eckert number |
| $M$ | magnetic parameter |
| $K$ | permeability parameter |
| $Kc$ | chemical reaction parameter |

*Greek symbols*

| | |
|---|---|
| $\omega_e$ | cyclotron frequency (e/mB) |
| $\tau_e$ | electron collision time (s) |
| $\sigma$ | electrical conductivity (sm$^{-1}$) |
| $\Omega$ | angular velocity (r/s) |
| $\nu$ | kinematic viscosity of the fluid (m$^2$ s$^{-1}$) |
| $\rho$ | fluid density (K gm$^{-3}$) |
| $\phi$ | non-dimensional concentration of the fluid |
| $\theta$ | non-dimensional temperature of the fluid |
| $\beta$ | coefficient of thermal expansion (K$^{-1}$) |
| $\beta^*$ | coefficient of mass expansion (m$^3$ Kg$^{-1}$) |

*Subscripts*

| | |
|---|---|
| $e$ | electron |
| $p$ | pressure |

in a rotating environment during past few decades due to their geophysical and astrophysical significance and their application in fluid engineering. Several important problems, namely, maintenance and secular variations of terrestrial magnetic field due to motion in Earth's liquid core, internal rotation rate of the sun, structure of rotating magnetic stars, planetary and solar dynamo problems, MHD Ekman pumping, turbo machines, rotating hydromagnetic generators, rotating drum type separator in closed cycle two phase MHD generator flow etc. are directly governed by the action of Coriolis and magnetic forces. An order of magnitude analysis shows that, in the hydromagnetic equations of motion in rotating environment, the effects of Coriolis force is more significant than that of inertial and viscous forces. In addition to it, Coriolis and magnetic forces are comparable in magnitude.

This study has applications in rotating magnetohydrodynamic (MHD) energy generators for new space systems and also thermal conversion mechanisms for nuclear propulsion space vehicles. The mechanism of conduction in ionized gases in the presence of a strong magnetic field is different from that in a metallic substance. The electric current in ionized gases is usually carried out by electrons which undergo successive collisions with other charged or neutral particles. It is to be noted that in the ionized gases, the current is proportional to the applied potential only when the electric field is very weak. However, in the presence of a strong electric field, the electrical conductivity is explicitly affected by the magnetic field. As a result of that, the conductivity parallel to the electric field is reduced. So, the current is reduced to the direction normal to both electric and magnetic fields. This phenomenon is known as the Hall effect (Cowling [34]). The effect of Hall current on MHD flows has been explored by several researchers owing to the application of such studies in the problems of MHD generators and Hall accelerators. It plays an important role in determining flow features of the fluid flow problems. It may be noted that Hall current induces secondary flow in fluid which is also characteristics of Coriolis force. Hall effects on fluid flow find applications in MHD power generation, nuclear power reactors and underground energy storage system and in several areas of astrophysics and geophysics. So it is appropriate to investigate the combined effects of Hall current and rotation on MHD fluid flow problems.

Datta and Jana [1] researched the Hall current effects on oscillatory magneto-hydrodynamic flow past a flat plate. Biswal and Sahoo [2] delienated the Hall current effects on oscillatory hydro-magnetic free convective flow of a visco-elastic fluid past an infinite vertical porous flat plate with mass transfer. Watanabe and Pop [3] demonstrated the Hall effects on a MHD boundary layer flow over a continuous moving flat plate. Aboeldahab and Elbarbary [4] probed the Hall current effect on a magneto- hydrodynamic free convection flow past a semi-infinite vertical plate with mass transfer. The Hall current effect with simultaneous thermal and mass diffusion on an unsteady hydro-magnetic flow near an accelerated vertical plate was studied by Acharya et al. [5]. Sharma et al. [6] presented the Hall effects on MHD mixed convective flow of a viscous incompressible fluid past a vertical porous plate, immersed in a porous medium with heat source/sink. Prabhakar Reddy and Anand Rao [7] showed radiation and thermal diffusion effects on an unsteady MHD

free convection mass transfer flow past an infinite vertical porous plate with Hall current and heat source. Raju et al. [8] displayed the Hall current effects on an unsteady MHD flow between a stretching sheet and an oscillating porous upper parallel plate with constant suction. Recently, Rajput and Kanaujia [9] researched on the MHD flow past a vertical plate with variable temperature and mass diffusion in the presence of Hall current. Veera Krishna et al. [10] made a discussion on the heat and mass transfer on unsteady MHD oscillatory flow of blood through porous arteriole. The effects of radiation and Hall current on an unsteady MHD free convective flow in a vertical channel filled with a porous medium have been studied by Veera Krishna et al. [11]. The heat generation/absorption and thermo-diffusion on an unsteady free convective MHD flow of radiating and chemically reactive second grade fluid near an infinite vertical plate through a porous medium and taking the Hall current into consideration have been studied by Veera Krishna and Chamkha [12]. Krishna and Reddy [14] examined the intricacies related to the unsteady MHD free convection in a boundary layer flow through porous medium. Krishna and Subba Reddy [15] discussed the replication on the MHD forced convective flow through stumpy permeable porous medium. The Hall effects on a visco-elastic fluid over an infinite oscillating porous plate with heat source and chemical reaction have been discussed by Krishna and Jyothi [16]. Reddy et al. [17] investigated MHD flow of nano-fluid through a saturating porous medium.

EL-Kabeir et al. [18] discussed an unsteady, three-dimensional, laminar, boundary-layer flow of a viscous, incompressible and electrically conducting fluid over inclined permeable surface embedded in porous medium in the presence of a uniform magnetic field and heat generation/absorption effects. Rashad et al. [19] investigated a steady, laminar, natural convection boundary-layer flow adjacent to a vertical cylinder embedded in a thermally stratified nanofluid-saturated non-Darcy porous medium. Chamkha et al. [20] considered unsteady, laminar, boundary-layer flow with heat and mass transfer of a nanofluid along a horizontal stretching plate in the presence of a transverse magnetic field, melting and heat generation or absorption effects. Bakier et al. [21] simulated a problem of hydromagnetic heat transfer by mixed convection along vertical plate in a liquid saturated porous medium in the presence of melting and thermal radiation effects for opposing external flow. Rashidi et al. [24] discussed viscous, laminar mixed convection boundary-layer flow over a horizontal plate, with chemical reaction. Rashidi et al., [25] investigated entropy generation on MHD Blood Flow of Nanofluid due to Peristaltic Waves. Stagnation point flow over a permeable shrinking sheet under the influence of MHD is analyzed using successive linearization method by Bhatti et al. [26]. Hamed and Rashidi [27] discussed A new analytical approach has been performed by using both similarity transformation and Variational Iteration Method (VIM) on the silver, copper, copper oxide, titanium oxide and aluminum oxide nanofluids flowing through a rotating channel with lower stretching porous wall under the squeezing MHD flow conditions. Rishidi et al. [28] investigated

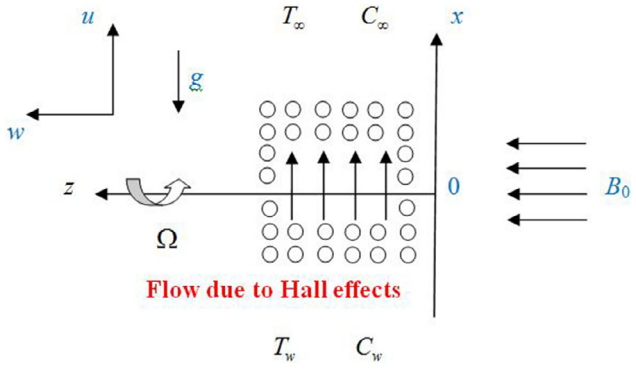


Fig. 1. Physical configuration of the problem.

the analysis of the second law of thermodynamics applied to an electrically conducting incompressible nanofluid fluid flowing over a porous rotating disk in the presence of an externally applied uniform vertical magnetic field. More recently, Veera Krishna and Chamkha [29] discussed the MHD squeezing flow of a water-based nanofluid through a saturated porous medium between two parallel disks, taking the Hall current into account. Veera Krishna et al. [30] discussed Hall effects on MHD peristaltic flow of Jeffrey fluid through porous medium in a vertical stratum. Veera Krishna et al. [31] discussed Hall effects on unsteady hydromagnetic natural convective rotating flow of second grade fluid past an impulsively moving vertical plate entrenched in a fluid inundated porous medium, while temperature of the plate has a temporarily ramped profile. Veera Krishna et al. [32] investigated the heat and mass transfer on MHD free convective flow over an infinite non-conducting vertical flat porous plate.

In this paper, we have studied Soret and Joule effects on MHD mixed convective two dimensional flow of an incompressible and electrically conducting viscous fluid past an infinite vertical porous plate. The salient features of the results are analyzed and discussed.

## 2. Formulation and solution of the problem

We have deemed the Hall effects on the mixed conventive flow of an incompressible and electrically conducting viscous fluid past an infinite vertical porous plate with Sore and Joule effects. We considered the Cartesian co-ordinate system such that $x$- axis is taken along the plate in upward direction and $z$- axis is normal to it (Fig. 1). The fluid and the plate rotate as a rigid body with a uniform angular velocity Ω about z-axis in the presence of an imposed uniform magnetic field $B_0$ normal to the plate. The induced magnetic field is tiny compared to external magnetic field. All the physical variables are independent of $x$. as the motion is two dimensional and length of the plate is large. A homogenous first order chemical reaction between fluid and the species concentration is taken into account in which the rate of chemical reaction is directly proportional to the species concentration.

The foremost and prevailing equations of continuity, momentum, energy and mass for a flow of an electrically

conducting fluid with respect to the rotating frame are

$$\frac{\partial w}{\partial z} = 0 \quad \Rightarrow w = \quad -w_0 \, (w_0 \; > 0) \tag{1}$$

$$w\frac{\partial u}{\partial z} + 2\Omega w = \nu\frac{\partial^2 u}{\partial z^2} + \frac{B_0 J_z}{\rho} - \frac{\nu}{k}u \; + g\beta(T - T_\infty) + g\beta^*(C - C_\infty) \tag{2}$$

$$w\frac{\partial w}{\partial z} - 2\Omega u = \nu\frac{\partial^2 w}{\partial z^2} - \frac{B_0 J_x}{\rho} - \frac{\nu}{k}w \tag{3}$$

$$w\frac{\partial T}{\partial z} = \frac{k_1}{\rho C_p}\frac{\partial^2 T}{\partial z^2} + \frac{\nu}{C_p}\left(\left(\frac{\partial u}{\partial z}\right)^2 + \left(\frac{\partial w}{\partial z}\right)^2\right) + \frac{\sigma B_0^2}{\rho C_p}\left(u^2 + w^2\right) + \frac{Q_0}{\rho C_p}(T - T_\infty) \tag{4}$$

$$w\frac{\partial C}{\partial z} = D\frac{\partial^2 C}{\partial z^2} + D_1\frac{\partial^2 T}{dz^2} - k_2(C - C_\infty) \tag{5}$$

The boundary conditions for the velocity, temperature and concentration fields are

$$u = 0, \; w = 0, \quad T = T_w, \quad C = C_w, \quad \text{at} \quad z = 0 \tag{6}$$

$$u = 0, \; w = 0, \quad T \to T_\infty, \quad C \to C_\infty, \quad \text{at} \quad z \; \to \infty \tag{7}$$

Lighthill [22] was the first to highlight the need to incorporate the Hall effect in MHD flows owing to the strong influence it can exert on flow distributions, for example in magnetic fusion systems, electrically-conducting aerodynamics, energy generators etc. Hall-magnetohydrodynamics (HMHD) takes into account this electric field description of MHD. The key difference from classical MHD studies is that in the absence of field line breaking, the magnetic field is tied to the electrons and not to the bulk fluid. When the strength of the magnetic field is very large, the generalized ohm's law is modified to include the hall current so that (Sutton and Sherman [23]),

$$J + \frac{\omega_e \tau_e}{B_0}(J \times B) = \sigma\left[E + V \times B + \frac{1}{e\eta_e}\nabla P_e\right] \tag{8}$$

The ion-slip and thermo electric effects are not included in Eq. (8). Further it is assumed that $\omega_e\tau_e \sim O(1)$. Also the electron pressure gradient, the ion-slip and thermoelectric effects are neglected. We also assume that the electric field $E = 0$ under these assumptions the Eq. (8) reduces to

$$J_x \; - m \; J_z = \; -\sigma B_0 w \tag{9}$$

$$J_z + m\, J_x = \sigma B_0 u \tag{10}$$

Where $m = \tau_e\omega_e$ is the Hall parameter.

On solving Eqs. (9) and (10) we obtain

$$J_x \; = \; \frac{\sigma B_0}{1 + m^2}(mu - w) \tag{11}$$

$$J_z \; = \frac{\sigma B_0}{1 + m^2}(u + mw) \tag{12}$$

Substituting the Eqs. (11) and (12) in (3) and (2), respectively, we obtain

$$w\frac{\partial u}{\partial z} + 2\Omega w = \nu\frac{\partial^2 u}{\partial z^2} + \frac{\sigma B_0^2(u + mw)}{\rho\left(1 + m^2\right)} - \frac{\nu}{k}u + g\beta(T - T_\infty) + g\beta^*(C - C_\infty) \tag{13}$$

$$w\frac{\partial w}{\partial z} - 2\Omega u = \nu\frac{\partial^2 w}{\partial z^2} - \frac{\sigma B_0^2(mu - w)}{\rho\left(1 + m^2\right)} - \frac{\nu}{k}w \tag{14}$$

Combining Eqs. (13) and (14), let $q = u + iw$ we obtain

$$w\frac{\partial q}{\partial z} + 2i\Omega q = \nu\frac{\partial^2 q}{\partial z^2} - \left(\frac{\sigma B_0^2}{\rho(1 + im)} + \frac{\nu}{k}\right)q + g\beta(T - T_\infty) + g\beta^*(C - C_\infty) \tag{15}$$

Introducing following non-dimensional quantities

$$z* = \frac{zw_0}{\nu}, \; q* = \frac{q}{w_0}, \; Pr = \frac{\nu\rho C_p}{k},$$
$$\theta = \frac{T - T_\infty}{T_w - T_\infty}, \; \phi = \frac{C - C_\infty}{C_w - C_\infty},$$
$$Gm = \frac{\nu g\beta^*(C_w - C_\infty)}{w_0^3}, \; Ec = \frac{w_0^2}{C_p(T_w - T_\infty)}, \; M^2 = \frac{\sigma B_0^2\nu}{\rho w_0^2},$$
$$R = \frac{\Omega\nu}{w_0^2}, \; K = \frac{\nu}{kw_0^2}, \; \nu = \frac{\mu}{\rho},$$
$$Sc = \frac{\nu}{D}, \; So = \frac{D_1(T_w - T_\infty)}{\nu(C_w - C_\infty)}, \; Gr = \frac{\nu g\beta(T_w - T_\infty)}{w_0^3},$$
$$Kr = \frac{\nu k_1}{w_0^2}, \quad Q = \frac{Q_o\nu}{\rho C_p w_0^2}$$

Making use of non-dimensional variables, we obtain the governing Eqs. (15), (4) and (5) in the dimensionless form as

$$\frac{d^2q}{dz^2} + \frac{dq}{dz} - \left(\frac{M^2}{1 + im} + \frac{1}{K} + 2iR\right)q = -Gr\theta - Gm\phi \tag{16}$$

$$\frac{d^2\theta}{dz^2} + \Pr\frac{d\theta}{dz} + \Pr Ec\left(\frac{\partial q}{\partial z}\right)^2 + \Pr Ec\, M^2 q^2 + \Pr Q\theta = 0 \tag{17}$$

$$\frac{d^2\phi}{dz^2} + Sc\frac{d\phi}{dz} - ScKc\phi + SoSc\frac{d^2\theta}{dz^2} = 0 \tag{18}$$

The corresponding boundary conditions in dimensionless form are reduced to

$$q = 0, \quad \theta = 1, \quad \phi = 1 \quad at \quad z = 0 \tag{19}$$

$$q \to 0, \quad \theta \to 0, \quad \phi \to 0 \quad at \quad z \to \infty \tag{20}$$

The physical variables $q$, $\theta$ and $\phi$ can be expanded in the power of Eckert number$Ec$. This can be possible physically as $Ec$ for the flow of an incompressible fluid is always less

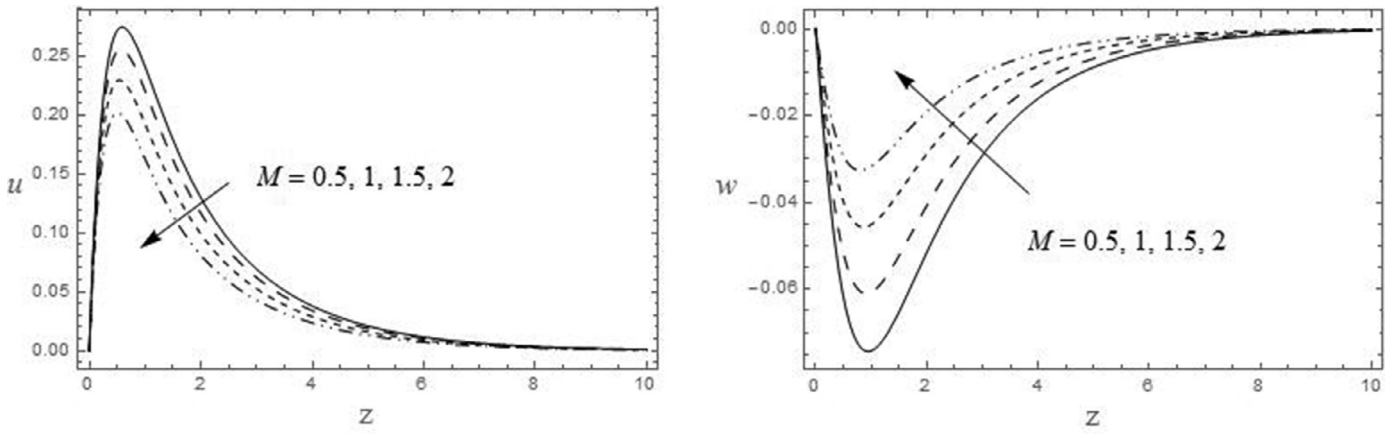


Fig. 2. The velocity profiles for $u$ and $w$ against $M$. $K = 0.5$, Pr $= 3$, $Gr = 3$, $Gm = 1$, $Q = 0.1$, $Kc = 1$, $Sc = 0.22$, $So = 0.5$, $m = 1, R = 0.5$.

than unity. It can be interrupted physically as the flow due to the Joules dissipation is super imposed on the main flow. Hence we can assume

$$\left.\begin{aligned} q(y) &= q_0(y) + Ecq_1(y) + O(Ec^2) \\ \theta(y) &= \theta_0(y) + Ec\theta_1(y) + O(Ec^2) \\ \phi(y) &= \phi_0(y) + Ec\phi_1(y) + O(Ec^2) \end{aligned}\right\} \tag{21}$$

Substituting the Eqs. (21) in Eqs. (16)–(18) and equating the coefficients of like powers of $Ec$, we have

$$\frac{d^2q_0}{dz^2} + \frac{dq_0}{dz} - \left(\frac{M^2}{1+im} + \frac{1}{K} + 2iR\right)q_0 = -Gr\theta_0 - Gm\phi_0 \tag{22}$$

$$\frac{d^2\theta_0}{dz^2} + \Pr\frac{d\theta_0}{dz} + \Pr Q\ \theta_0 = 0 \tag{23}$$

$$\frac{d^2\phi_0}{dz^2} + Sc\frac{d\phi_0}{dz} - KcSc\phi_0 = -SoSc\frac{d^2\theta_0}{dz^2} \tag{24}$$

$$\frac{d^2q_1}{dz^2} + \frac{dq_1}{dz} - \left(\frac{M^2}{1+im} + \frac{1}{K} + 2iR\right)q_1 = -Gr\theta_1 - Gm\phi_1 \tag{25}$$

$$\frac{d^2\theta_1}{dz^2} + \Pr\frac{d\theta_1}{dz} + \Pr Q\theta_1 = -\Pr\left(\frac{dq_0}{dz}\right)^2 - \Pr M^2q_0^2 \tag{26}$$

$$\frac{d^2\phi_1}{dz^2} + Sc\frac{d\phi_1}{dz} - ScKc\phi_1 = -SoSc\frac{d^2\theta_1}{dz^2} \tag{27}$$

And the corresponding boundary conditions are

$$\begin{aligned} &q_0 = 0,\ \ q_1 = 0,\ \ \theta_0 = 1,\ \ \theta_1 = 0, \\ &\phi_0 = 1,\ \ \phi_1 = 0 \qquad at \qquad z = 0 \end{aligned} \tag{28}$$

$$\begin{aligned} &q_0 \to 0,\ q_1 \to 0,\ \theta_0 \to 0,\ \theta_1 \to 0,\ \phi_0 \to 0, \\ &\phi_1 \to 0 \quad at \quad z \to \infty \end{aligned} \tag{29}$$

Solving Eqs. (22)–(27) with the help of boundary conditions (28) and (29), we obtain the velocity, temperature and concentration distributions in the boundary layer.

For engineering interest, the coefficient of skin-friction at the plate, the rate of heat transfer coefficient in terms of the Nusselt number and the rate of mass transfer coefficient in terms of the Sherwood number in non-dimensional form are obtained by

$$C_f = \left(\frac{\partial u}{\partial z}\right)_{z=0} \ ;\ \ Nu = \left(\frac{\partial\theta}{\partial z}\right)_{z=0} \ \ and \ \ \ Sh = \left(\frac{\partial\phi}{\partial z}\right)_{z=0} \tag{30}$$

Where, some expressions and constants are mentioned in Appendix.

## 3. Results and discussion

In the present study, the following default parameter values are adopted for computations: $m = 1$, $R = 0.5$, $Gr = 3$, $Gm = 1$, $K = 0.5$, $M = 0.5$, Pr $= 3$, $Ec = 0.01$, $Q = 0.1$, $Sc = 0.6$, $Kr = 0.1$, $So = 0.5$. All graphs therefore correspond to these values unless specifically indicated in the appropriate graph. Figs. 2–12, Figs. 13, and 14 depict the velocity, temperature and concentration distributions respectively. Tables (1–3) represent variation in Skin friction, Nusselt number and Sherwood number.

From the Fig. 2, we observed that the primary and secondary velocity components $u$ and $w$ get reduced when the intensity of the magnetic field $M$ is increased. This is due to the fact that the introduction of a transverse magnetic field, normal to the flow direction, has a tendency or affinity to create the drag known as the Lorentz force which tends to resist the flow. The resultant velocity is also reduced with increasing Hartmann number $M$. It is observed from the Fig. 3, that as the permeability parameter $K$ is increased, both the velocity components $u$ and $w$ is increased. Lower the permeability lesser the fluid speed is observed in the entire fluid region. The resultant velocity is also enhanced with increasing $K$. The influence of Prandtl number Pr and heat generation parameter $Q$ on the dimensionless velocity components

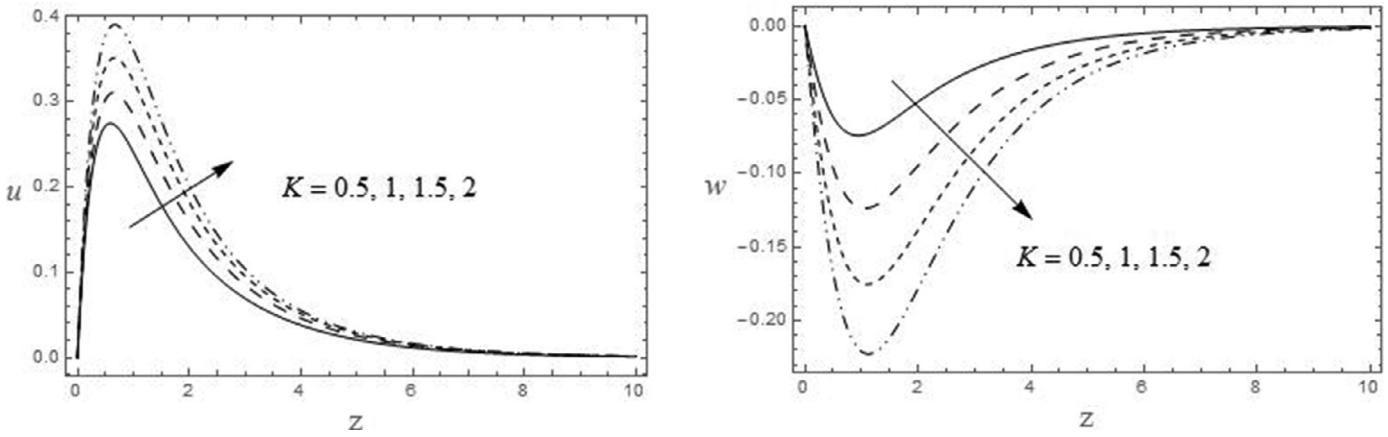


Fig. 3. The velocity profiles for $u$ and $w$ against $K$. $M = 0.5$, Pr $= 3$, $Gr = 3$, $Gm = 1$, $Q = 0.1$, $Kc = 1$, $Sc = 0.22$, $So = 0.5$, $m = 1, R = 0.5$.

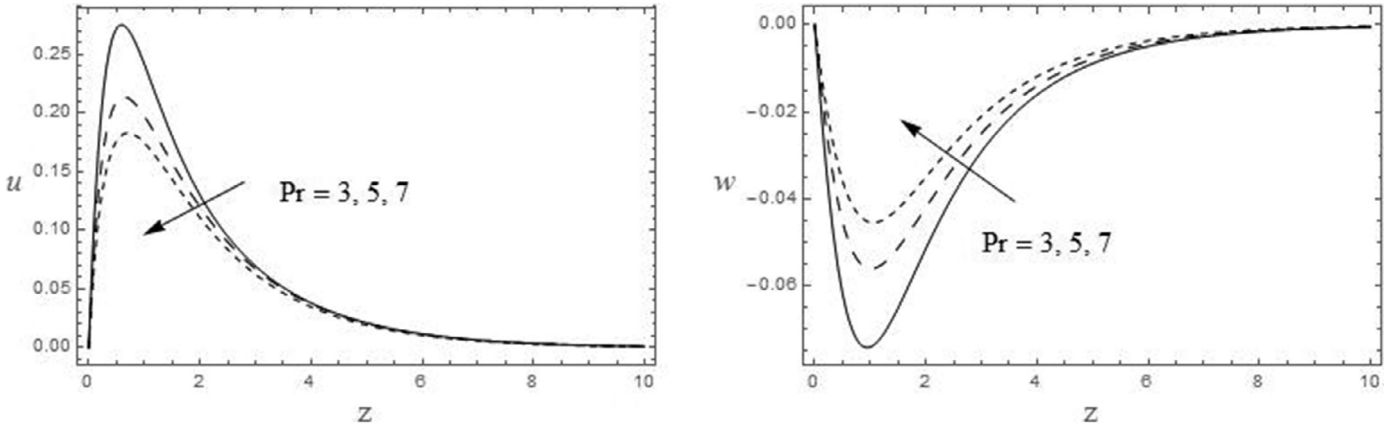


Fig. 4. The velocity profiles for $u$ and $w$ against Pr. $M = 0.5$, $K = 0.5$, $Gr = 3$, $Gm = 1$, $Q = 0.1$, $Kc = 1$, $Sc = 0.22$, $So = 0.5$, $m = 1, R = 0.5$.

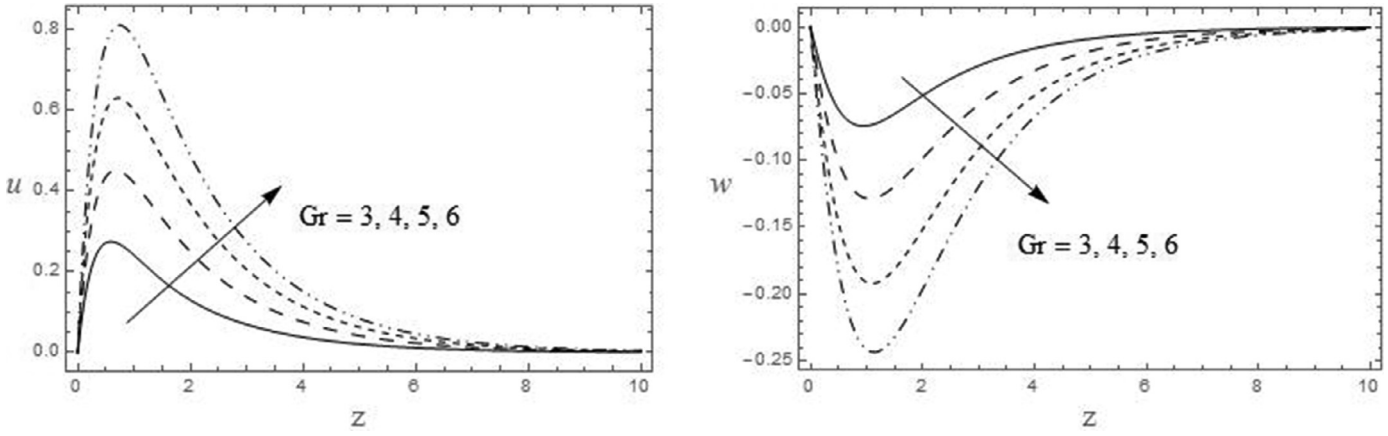


Fig. 5. The velocity profiles for $u$ and $w$ against Gr. $M = 0.5$, $K = 0.5$, Pr $= 3$, $Gm = 1$, $Q = 0.1$, $Kc = 1$, $Sc = 0.22$, $So = 0.5$, $m = 1, R = 0.5$.

$u$ and $w$ for the fixed values of other parameters is shown in Figs. 4 and 8. It is noticed that both the dimensionless velocity components $u$ and $w$ decrease with Pr and increase with $Q$. The thermal Grashof number Gr signifies the relative effect of the thermal buoyancy force to the viscous hydrodynamic force in the boundary layer. Fig. 5 presents the effects of Gr on the velocity components $u$ and $w$ for the fixed values of other parameters. It is observed that the dimensionless velocity increases with increasing Gr. The mass Grashof number Gm defines the ratio of the species buoyancy force to the viscous hydrodynamic force. Fig. 6 exhibits the effect of Gm on the dimensionless velocity components $u$ and $w$. It is noticed that the primary and secondary velocities increase with increasing mass Grashof number Gm. The resultant velocity

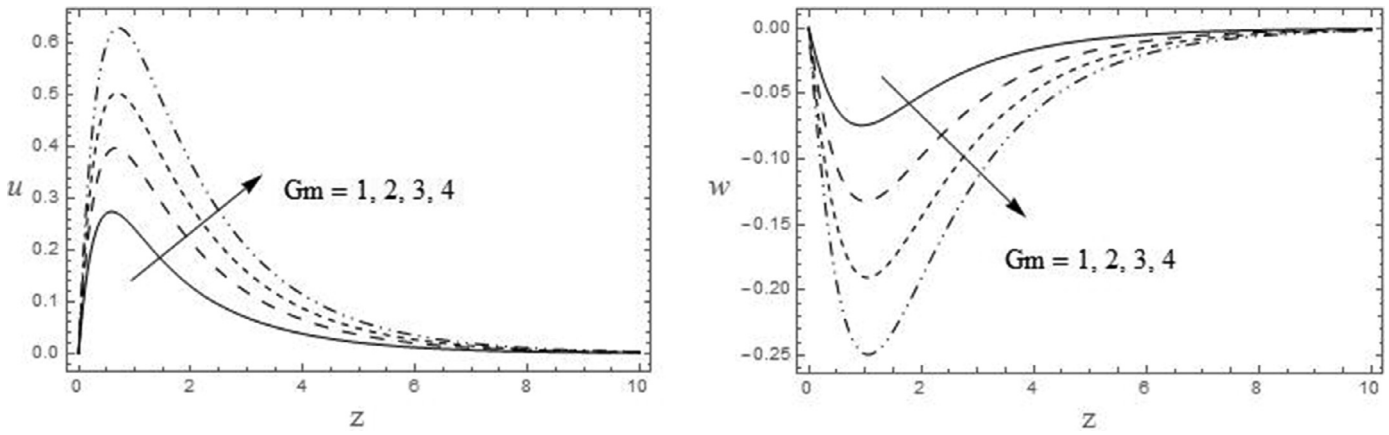


Fig. 6. The velocity profiles for $u$ and $w$ against Gm. $M = 0.5$, $K = 0.5$, Pr $= 3$, $Gr = 3$, $Q = 0.1$, $Kc = 1$, $Sc = 0.22$, $So = 0.5$, $m = 1, R = 0.5$.

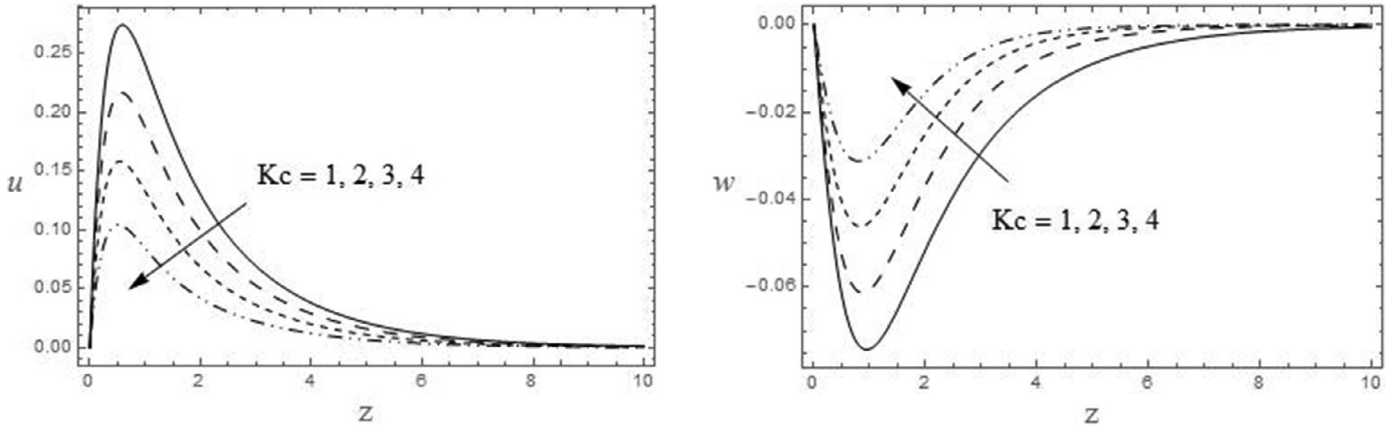


Fig. 7. The velocity profiles for $u$ and $w$ against Kc. $M = 0.5$, $K = 0.5$, Pr $= 3$, $Gr = 3$, $Gm = 1$, $Q = 0.1$, $Sc = 0.22$, $So = 0.5$, $m = 1, R = 0.5$.

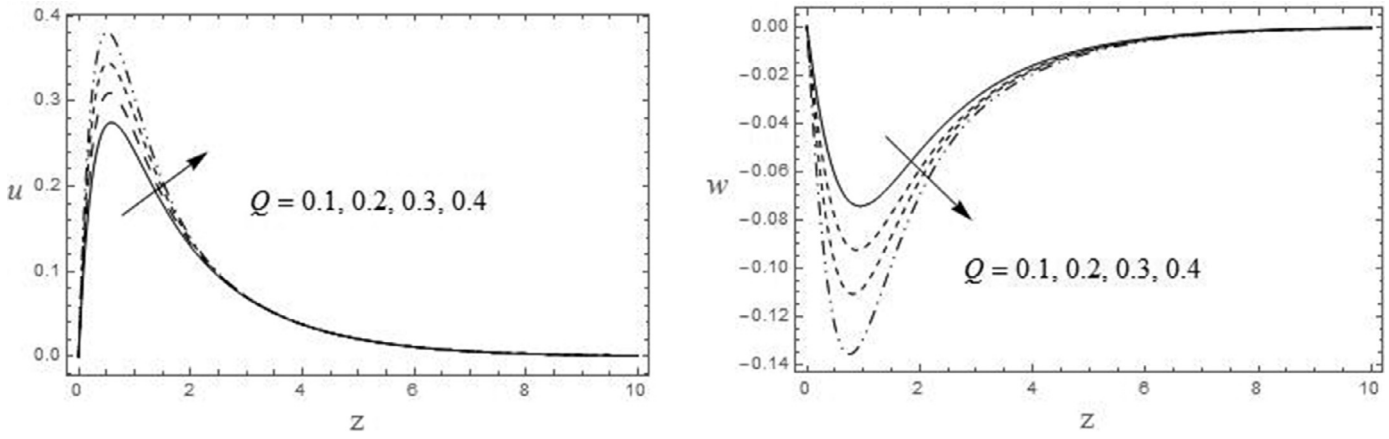


Fig. 8. The velocity profiles for $u$ and $w$ against $Q$. $M = 0.5$, $K = 0.5$, Pr $= 3$, $Gr = 3$, $Gm = 1$, $Kc = 1$, $Sc = 0.22$, $So = 0.5$, $m = 1, R = 0.5$.

is also increases with increasing Gr or Gm throughout the fluid region. Fig. 7 illustrates the effects of chemical reaction parameter Kc on the velocity components $u$ and $w$ for the fixed values of other parameters. It is observed that the primar and secondary velocity components $u$ and $w$ decrease with increasing Kc. The resultant velocity is also decreases with increasing Kc throughout the fluid region. Figs. 9 and 10 are prepared to show the influence of Schmidt number Sc and Soret parameter $So$ on the primar and secondary velocity components $u$ and $w$. It is found that there is slightly decrease and an increase in the both primary and secondary velocity components $u$ and $w$ with Sc and $So$, respectively. The resultant velocity also decreases and increases with increasing Sc and $So$ throughout the fluid region. From Fig. 11 both the

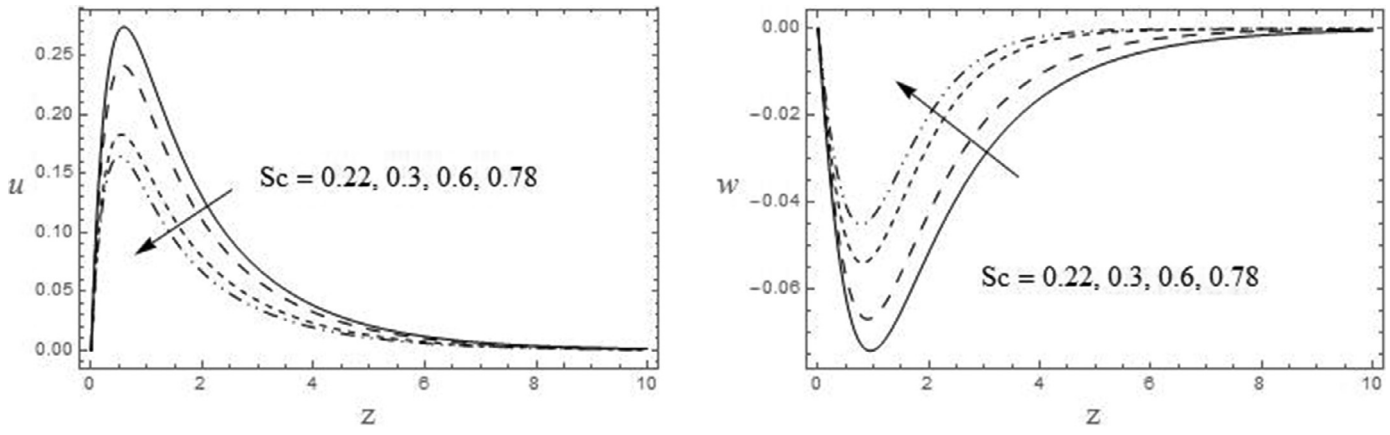


Fig. 9. The velocity profiles for $u$ and $w$ against Sc. $M = 0.5$, $K = 0.5$, Pr $= 3$, $Gr = 3$, $Gm = 1$, $Q = 0.1$, $Kc = 1$, $So = 0.5$, $m = 1, R = 0.5$.

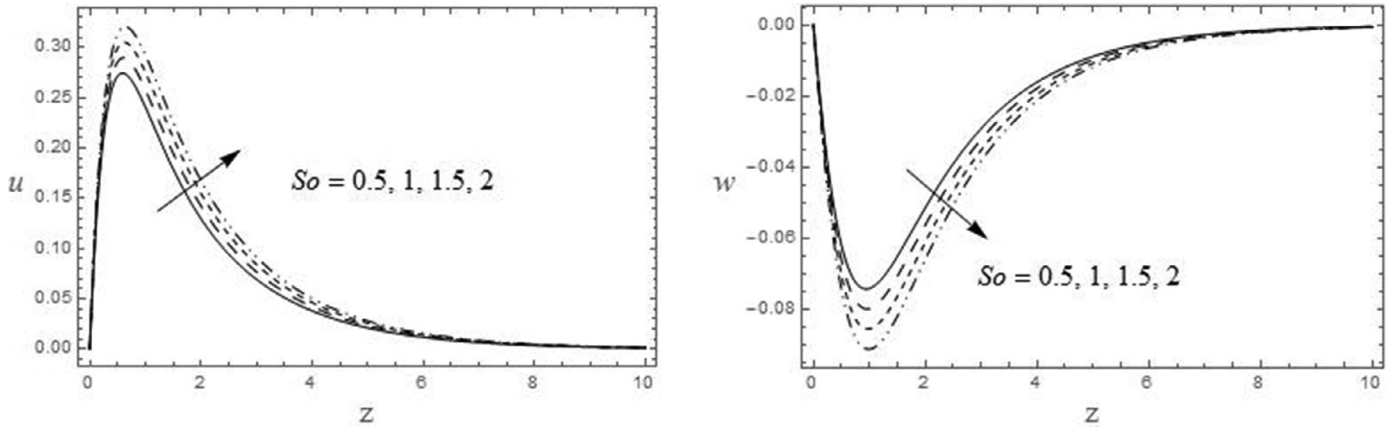


Fig. 10. The velocity profiles for $u$ and $w$ against $So$. $M = 0.5$, $K = 0.5$, Pr $= 3$, $Gr = 3$, $Gm = 1$, $Q = 0.1$, $Kc = 1$, $Sc = 0.22$, $m = 1$, $R = 0.5$.

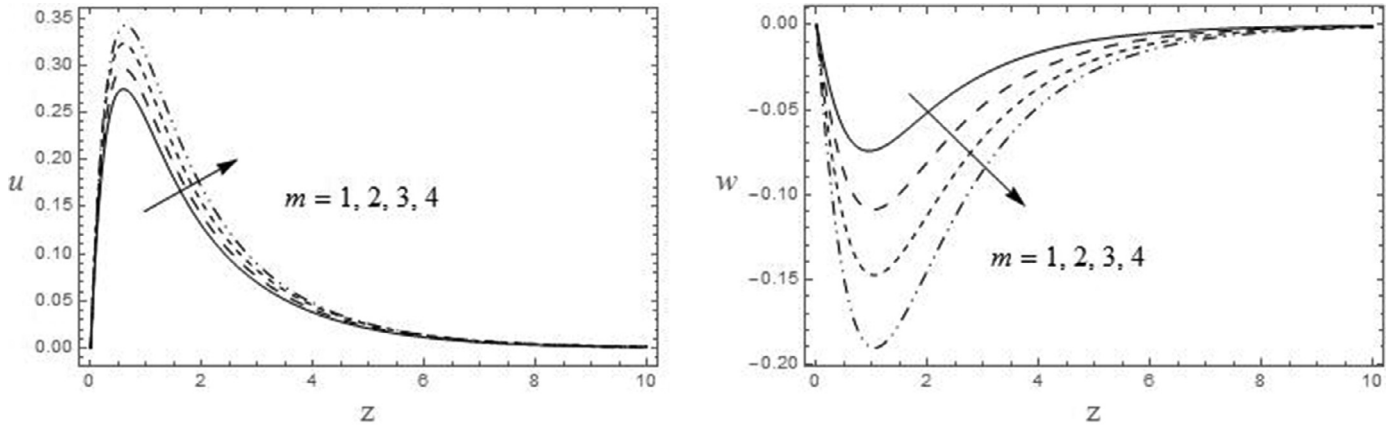


Fig. 11. The velocity profiles for $u$ and $w$ against $m$. $M = 0.5$, $K = 0.5$, Pr $= 3$, $Gr = 3$, $Gm = 1$, $Q = 0.1$, $Kc = 1$, $Sc = 0.22$, $So = 0.5$, $R = 0.5$.

velocity components $u$ and $w$ are enhanced with increasing Hall parameter $m$. The resultant velocity also increases with increasing Hall parameter throughout the fluid region. The similar behaviour is observed with increasing rotation parameter $E$ (Fig. 12).

The persuade of Prandtl number Pr, heat generation parameter $Q$, Hartmann number $M$ and Eckert number $Ec$ on the dimensionless temperature for the fixed values of other parameters is shown in Fig. 13, respectively. The temperature reduces with increasing Prandtl number Pr and enhances with

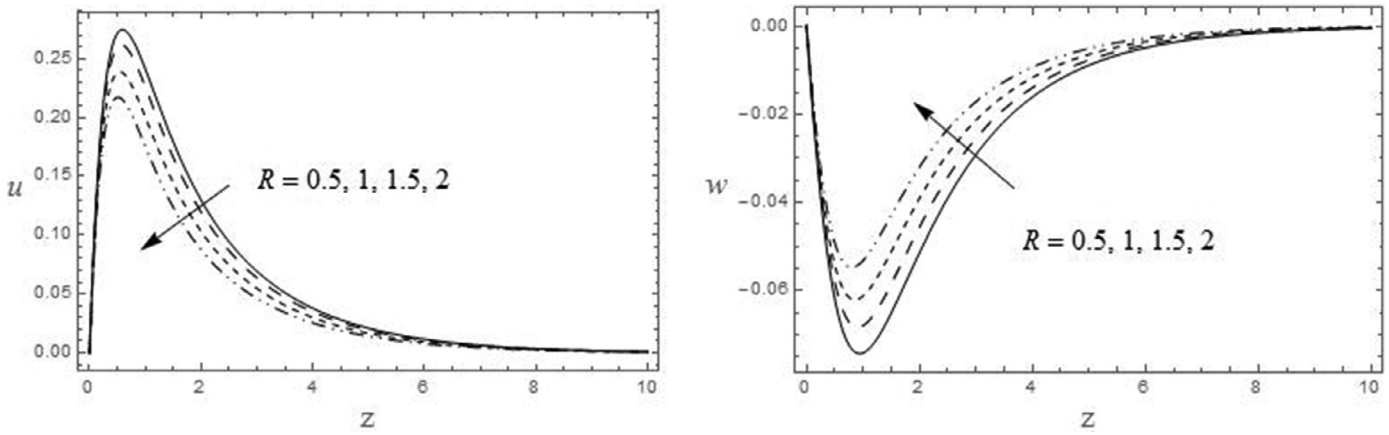


Fig. 12. The velocity profiles for $u$ and $w$ against $R$. $M = 0.5$, $K = 0.5$, $m = 1$, $\mathrm{Pr} = 3$, $Gr = 3$, $Gm = 1$, $Q = 0.1$, $Kc = 1$, $Sc = 0.22$, $So = 0.5$.

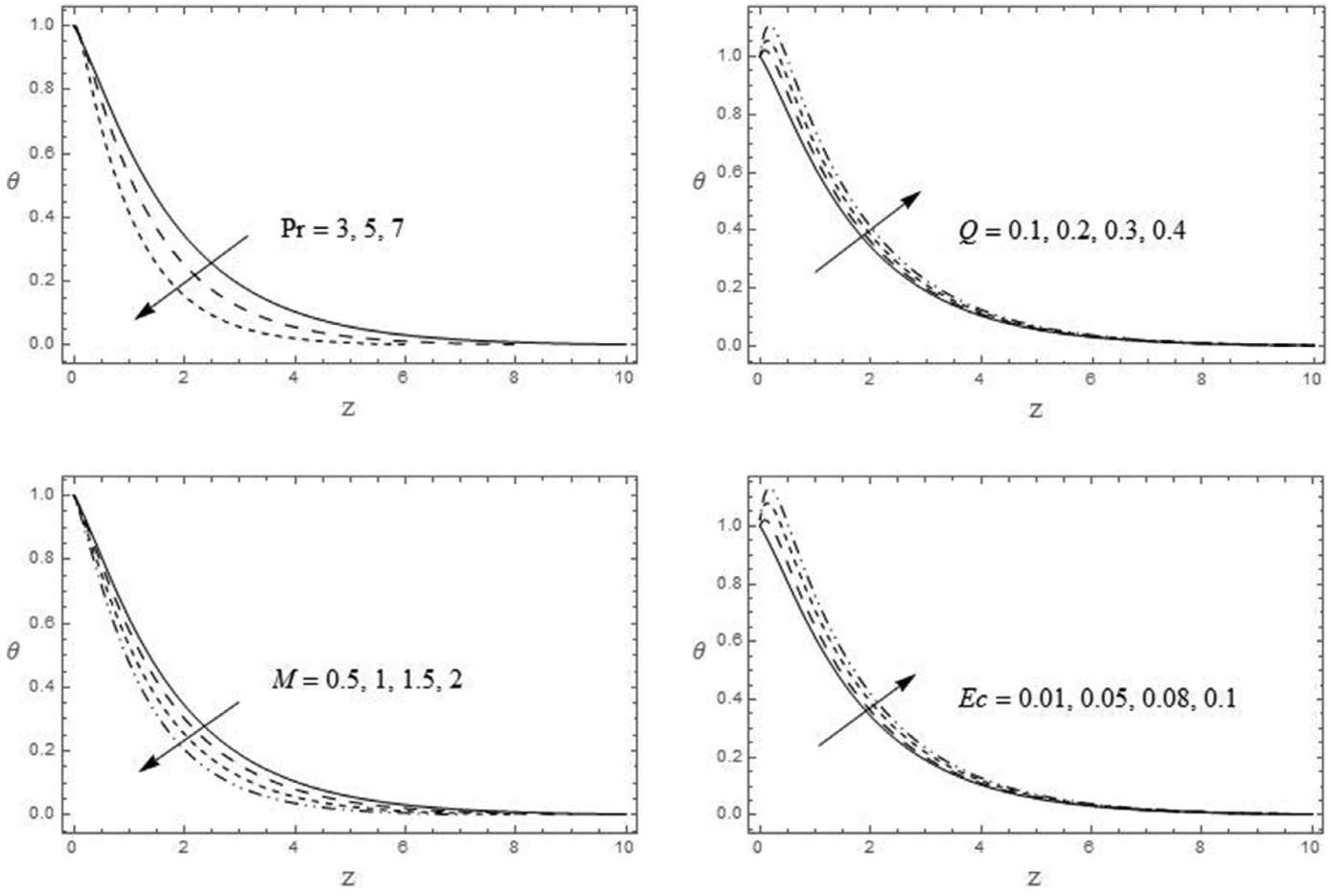


Fig. 13. The temperature profile for $\theta$ against Pr, $Q$, $M$ and $Ec$.

increasing heat generation parameter $Q$. Likewise the temperature retards with increase in $M$ and enhances with increase in $Ec$ throughout the fluid region.

Figs. 14 displayed the result of the dimensionless concentration for various values of chemical reaction parameter Kc, Schmidt number Sc and Soret parameter $So$ and Eckert number $Ec$. It is clear from the figure that the concentration profiles decrease with the increase of Kc. This shows that the buoyancy effects (due to concentration and temperature difference) are important in the plate. Moreover it is observed that the fluid motion is retarded on the account of chemical reaction. This shows that the destructive reaction $\mathrm{Kc} > 0$ leads to fall in the concentration field which in turn weakens the buoyancy effects due to concentration gradients. It is found

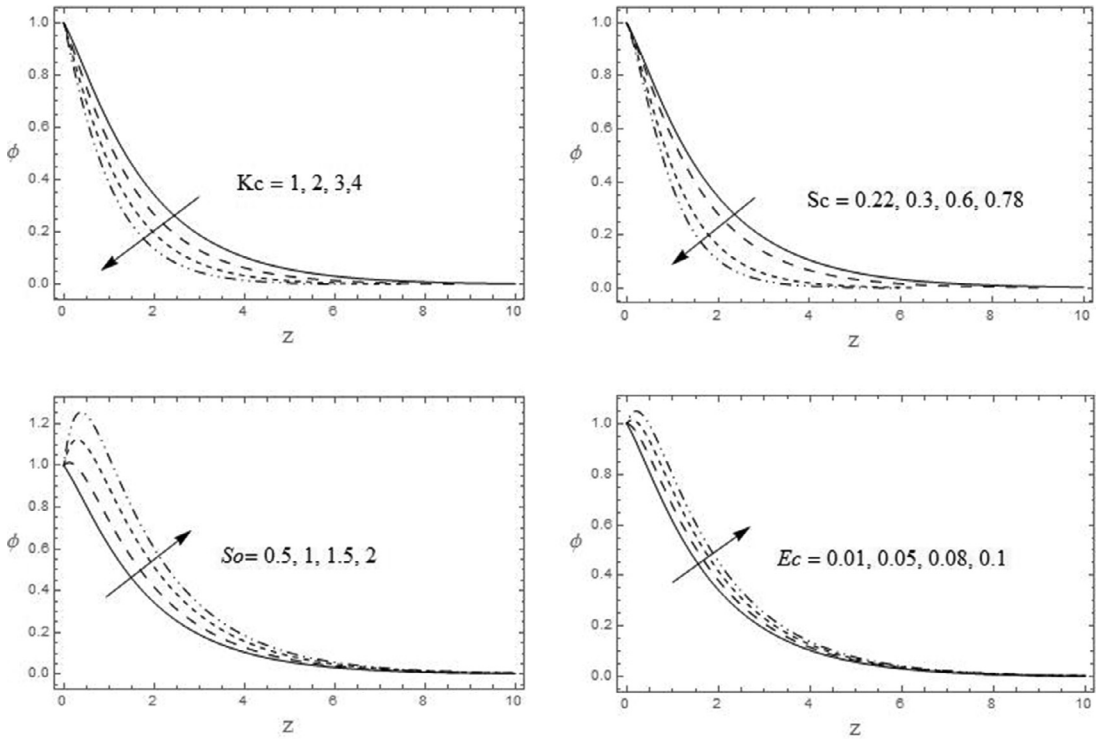


Fig. 14. The Concentration profiles for $\phi$ against Kc, Sc, *So* and *Ec*.

Table 1
Shear stress. ($Ec = 0.01$).

| *M* | *K* | *R* | Pr | Gr | Gm | Kc | *Q* | Sc | *So* | *m* | $\lvert \tau \rvert$ |
|---|---|---|---|---|---|---|---|---|---|---|---|
| 0.5 | 0.5 | 0.5 | 3 | 3 | 1 | 1 | 0.1 | 0.22 | 0.5 | 1 | 1.41365 |
| 1 | | | | | | | | | | | 1.35316 |
| 1.5 | | | | | | | | | | | 1.26409 |
| | 1 | | | | | | | | | | 1.69782 |
| | 1.5 | | | | | | | | | | 1.85738 |
| | | 1 | | | | | | | | | 1.36654 |
| | | 1.5 | | | | | | | | | 1.27048 |
| | | | 5 | | | | | | | | 1.17022 |
| | | | 7 | | | | | | | | 1.04676 |
| | | | | 4 | | | | | | | 1.67454 |
| | | | | 5 | | | | | | | 1.92973 |
| | | | | | 2 | | | | | | 2.07856 |
| | | | | | 3 | | | | | | 2.73871 |
| | | | | | | 2 | | | | | 1.34858 |
| | | | | | | 3 | | | | | 1.30323 |
| | | | | | | | 0.3 | | | | 1.46711 |
| | | | | | | | 0.5 | | | | 1.53702 |
| | | | | | | | | 0.3 | | | 1.38647 |
| | | | | | | | | 0.6 | | | 1.30918 |
| | | | | | | | | | 1 | | 1.46371 |
| | | | | | | | | | 1.5 | | 1.50777 |
| | | | | | | | | | | 2 | 1.43480 |
| | | | | | | | | | | 3 | 1.44855 |

that there is decrease and an increase in the concentration with increasing Sc and *So* or *Ec*, respectively.

The variation in skin-friction coefficient, the rate of heat transfer in the form of Nusselt number and the rate of mass transfer in the form of Sherwood number for various parameters are studied through Tables 1–3. Skin friction coefficient reduces with increasing Hartmann number M, rotation parameter *R*, Prandtl number Pr, chemical reaction parameter Kc and Schmidt number Sc; similarly it enhances permeability parameter K, thermal Grashof number Gr, mass

Table 2
Nusselt number. ($Kc = 1$, $R = 0.5$, $So = 0.5$, $Sc = 0.6$, $Ec = 0.01$).

| $M$ | $K$ | $m$ | Gr | Gm | Pr | $Q$ | Nu |
|---|---|---|---|---|---|---|---|
| 0.5 | 0.5 | 1 | 3 | 1 | 3 | 0.1 | −2.88732 |
| 1.0 | | | | | | | −2.88600 |
| 1.5 | | | | | | | −2.88501 |
| | 1.0 | | | | | | −2.88076 |
| | 1.5 | | | | | | −2.87585 |
| | | 2 | | | | | −2.88702 |
| | | 3 | | | | | −2.88692 |
| | | | 4 | | | | −2.88455 |
| | | | 5 | | | | −2.88136 |
| | | | | 2 | | | −2.87350 |
| | | | | 3 | | | −2.85308 |
| | | | | | 4 | | −4.88828 |
| | | | | | 5 | | −6.88757 |
| | | | | | | 0.2 | −2.77458 |
| | | | | | | 0.3 | −2.65081 |

Table 3
Sherwood number. (Pr = 3, $R = 0.5$, $Gr = 3$, $Gm = 1$, $Q = 0.1$, $Ec = 0.01$).

| $M$ | $K$ | $m$ | Gm | $So$ | Sc | Kc | Sh |
|---|---|---|---|---|---|---|---|
| 0.5 | 0.5 | 1 | 1 | 0.5 | 0.22 | 1 | −0.310393 |
| 1.0 | | | | | | | −0.310530 |
| 1.5 | | | | | | | −0.310632 |
| | 1.0 | | | | | | −0.311101 |
| | 1.5 | | | | | | −0.311630 |
| | | 2 | | | | | −0.310425 |
| | | 3 | | | | | −0.310436 |
| | | | 2 | | | | −0.311889 |
| | | | 3 | | | | −0.314097 |
| | | | | 1 | | | −0.029212 |
| | | | | 1.5 | | | −0.008759 |
| | | | | | 0.3 | | −0.339451 |
| | | | | | 0.6 | | −0.398348 |
| | | | | | | 2 | −0.516411 |
| | | | | | | 3 | −0.674663 |

Grashof number Gm, heat generation parameter $Q$ and soret parameter $So$ (Table 1). The magnitude of the Nusselt number $Nu$ increases with increasing Prandtl number Pr and reverse trend with increasing Hartmann number $M$, permeability parameter $K$, Hall parameter $m$, thermal Grashof number Gr, mass Grashof number Gm or heat generation parameter $Q$ (Table 2). In the same manner, the magnitude of the Sherwood number $Sh$ increases with increasing Hartmann number $M$, permeability parameter $K$, Hall parameter $m$, mass Grahof number Gm, Schmidt number Sc or Chemical reaction parameter Kc and reduces with increasing Soret parameter $So$. For the validity of our work we have compared our results with the existing results of Reddy et al. [25] in the absence of porous medium and heat source. Our result appears to be in line, in sync with or in tremendous agreement with the existing results (Table 4).

## 4. Conclusions

We have considered the Soret and Joule effects of MHD mixed convective flow of an incompressible and electrically conducting viscous fluid past an infinite vertical porous plate taking Hall effects into account. Mathematical analysis is through and the upshots are,

1. The concentration distribution increases with increase in Soret number and decreases with the chemical reaction effect.
2. The resultant velocity increases with an increase in Hall parameter or thermal Grashof number or mass Grashof number.
3. As the intensity of the magnetic field increases, the resultant velocity decreases.
4. Both the resultant velocity and concentration of fluid decrease with increase of Schmidt number.
5. An increase in Prandtl number results in the decrease in temperature distribution.
6. Both the resultant velocity and dimensionless temperature are increasing according to the increasing values of heat source parameter.
7. Skin friction coefficient decreases with an increase in Hartmann number or permeability parameter, whereas it shows reverse effect in the case of thermal Grashof number and mass Grashof number.
8. Nusselt number increases with the increase in Prandtl number.
9. Sherwood number increases with increasing Schmidt number or Chemical reaction parameter and reduces with increasing Soret parameter.

Table 4
Comparison of results. ($K = \infty$, $m = 0$, $R = 0$, $Gr = 3$, $Gm = 1$, Pr = 3, $Q = 0$, $Ec = 0.01$).

| $M$ | Kc | $So$ | Sc | Reddy et al. [13] | | | Present work | | |
|---|---|---|---|---|---|---|---|---|---|
| | | | | $C_f$ | $Nu$ | $Sh$ | $C_f$ | $Nu$ | $Sh$ |
| 0.5 | 1 | 0.5 | 0.22 | 2.32043 | −0.96211 | −0.30228 | 2.32041 | −0.96208 | −0.30225 |
| 1 | | | | 1.73126 | −2.97742 | −0.30062 | 1.73124 | −2.97739 | −0.30059 |
| 1.5 | | | | 1.37982 | −2.98525 | −0.29978 | 1.37980 | −2.98522 | −0.29974 |
| | 2 | | | 2.04400 | −2.97446 | −0.50725 | 2.04398 | −2.97442 | −0.50721 |
| | 3 | | | 1.89559 | −2.97974 | −0.66515 | 1.89557 | −2.97970 | −0.66510 |
| | | 1 | | 2.43803 | −2.95646 | −0.01399 | 2.43801 | −2.95641 | −0.01394 |
| | | 1.5 | | 2.55580 | −2.95043 | 0.27308 | 2.55577 | −2.95038 | 0.27303 |
| | | | 0.3 | 2.16276 | −2.96972 | −0.32741 | 2.16275 | −2.96968 | −0.32736 |
| | | | 0.6 | 1.86766 | −2.98089 | −0.37159 | 1.86764 | −2.98084 | −0.37154 |

## Appendix

$$q_0 = a_5e^{-m_3z} + a_4e^{-m_2z} + a_3e^{-m_1z},\ \theta_0 = e^{-m_1z},$$
$$\phi_0 = a_2e^{-m_2z} + a_1e^{-m_1z}$$
$$q_1 = a_{29}e^{-m_6z} + a_{21}e^{-m_5z} + a_{22}e^{-m_4z} + a_{23}e^{-2m_3z} + a_{24}e^{-2m_2z} + a_{25}e^{-2m_1z} + a_{26}e^{-(m_3+m_2)z} + a_{27}e^{-(m_1+m_2)z} + a_{28}e^{-(m_1+m_3)z}$$

$$\theta_1 = a_{12}e^{-m_4z} + a_6e^{-2m_3z} + a_7e^{-2m_2z} + a_8e^{-2m_1z} + a_9e^{-(m_3+m_2)z} + a_{10}e^{-(m_1+m_2)z} + a_{11}e^{-(m_1+m_3)z}$$
$$\phi_1 = a_{20}e^{-m_5z} + a_{13}e^{-m_4z} + a_{14}e^{-2m_3z} + a_{15}e^{-2m_2z} + a_{16}e^{-2m_1z} + a_{17}e^{-(m_3+m_2)z} + a_{18}e^{-(m_1+m_2)z} + a_{19}e^{-(m_1+m_3)z}$$

$$C_f = -(m_3a_5 + m_2a_4 + m_1a_3) - Ec\ (m_6a_{29} + m_5a_{21} + m_4a_{22} + 2m_3a_{23} + 2m_2a_{24} + 2m_1a_{25} + (m_3+m_2)a_{26} + (m_1+m_2)a_{27} + (m_3+m_1)a_{28})$$

$$Nu = -m_1 - Ec\ (m_4a_{12} + 2m_3a_6 + 2m_2a_7 + 2m_1a_8 + (m_3+m_2)a_9 + (m_1+m_{22})a_{10} + (m_3+m_{21})a_{11})$$
$$Sh = -(m_1a_2 + m_1a_1) - Ec(m_5a_{20} + m_4a_{13} + 2m_3a_{14} + 2m_2a_{15} + 2m_1a_{16} + (m_3+m_2)a_{17} + (m_1+m_2)a_{18} + (m_3+m_1)a_{19})$$

$$m_1 = \frac{\Pr + \sqrt{\Pr^2 - 4Q\Pr}}{2},\quad m_2 = \frac{Sc + \sqrt{Sc^2 + 4KcSc}}{2},$$
$$m_3 = \frac{1 + \sqrt{1 + 4\left(\frac{M^2}{1+im} + \frac{1}{K} + 2iR\right)}}{2},$$
$$m_4 = \frac{-\Pr + \sqrt{\Pr^2 - 4Q\Pr}}{2},\quad m_5 = \frac{-Sc + \sqrt{Sc^2 + 4KcSc}}{2},$$
$$m_6 = \frac{-1 + \sqrt{1 + 4\left(\frac{M^2}{1+im} + \frac{1}{K} + 2iR\right)}}{2},$$

$$a_1 = \frac{-SoScm_1^2}{m_1^2 - Scm_1 - KcSc},\quad a_2 = 1 - a_1,$$
$$a_3 = \frac{-(A_1Gm + Gr)}{m_1^2 - m_1 - \left(\frac{M^2}{1+im} + \frac{1}{K} + 2iR\right)},$$
$$A_4 = \frac{-A_2Gm}{m_2^2 - m_2 - \left(\frac{M^2}{1+im} + \frac{1}{K} + 2iR\right)},\quad A_5 = -A_4 - A_3,$$
$$A_6 = \frac{-\Pr A_5^2(m_3^2 + M^2)}{4m_3^2 - 2\Pr m_3 + \Pr Q},$$
$$a_7 = \frac{-\Pr A_4^2(m_2^2 + M^2)}{4m_2^2 - 2\Pr m_2 + \Pr Q},\ a_8 = \frac{-\Pr A_3^2(m_1^2 + M^2)}{4m_1^2 - 2\Pr m_1 + \Pr Q},$$
$$a_9 = \frac{-2\Pr A_4A_5(m_3m_2 + M^2)}{(m_3+m_2)^2 - \Pr(m_3+m_2) + \Pr Q},$$
$$a_{10} = \frac{-2\Pr A_3A_4(m_1m_2 + M^2)}{(m_1+m_2)^2 - \Pr(m_1+m_2) + \Pr Q},$$
$$a_{11} = \frac{-2\Pr a_3a_5(m_3m_1 + M^2)}{(m_3+m_1)^2 - \Pr(m_3+m_1) + \Pr Q},$$
$$a_{12} = -a_{11} - a_{10} - a_9 - a_8 - a_7 - a_6,$$
$$a_{13} = \frac{-SoScm_4^2a_{12}}{m_4^2 - Scm_4 - KcSc},\ a_{14} = \frac{-4SoScm_3^2a_6}{4m_3^2 - 2Scm_3 - KcSc},$$
$$a_{15} = \frac{-4SoScm_2^2a_7}{4m_2^2 - 2Scm_2 - KcSc},$$
$$a_{16} = \frac{-4SoScm_1^2a_8}{4m_1^2 - 2Scm_1 - KcSc},$$
$$a_{17} = \frac{-SoSc(m_3+m_2)^2a_9}{(m_3+m_2)^2 - Sc(m_3+m_2) - KcSc},$$
$$a_{18} = \frac{-SoSc(m_1+m_2)^2a_{10}}{(m_1+m_2)^2 - Sc(m_1+m_2) - KcSc},$$
$$a_{19} = \frac{-SoSc(m_3+m_1)^2a_{11}}{(m_3+m_1)^2 - Sc(m_3+m_1) - KcSc},$$
$$a_{20} = -a_{13} - a_{14} - a_{15} - a_{16} - a_{17} - a_{18} - a_{19},$$
$$a_{21} = \frac{-a_{20}Gm}{m_5^2 - m_5 - \left(\frac{M^2}{1+im} + \frac{1}{K} + 2iR\right)},$$
$$a_{22} = \frac{(-a_{13}Gm - A_{12}Gr)}{m_4^2 - m_4 - \left(\frac{M^2}{1+im} + \frac{1}{K} + 2iR\right)},$$
$$a_{23} = \frac{(-a_6Gr - A_{14}Gm)}{4m_3^2 - 2m_3 - \left(\frac{M^2}{1+im} + \frac{1}{K} + 2iR\right)},$$
$$a_{24} = \frac{(-a_7Gr - a_{15}Gm)}{4m_2^2 - 2m_2 - \left(\frac{M^2}{1+im} + \frac{1}{K} + 2iR\right)},$$
$$a_{25} = \frac{(-a_8Gr - a_{16}Gm)}{4m_1^2 - 2m_1 - \left(\frac{M^2}{1+im} + \frac{1}{K} + 2iR\right)},$$
$$a_{26} = \frac{(-a_{17}Gm - a_9Gr)}{(m_3+m_2)^2 - (m_3+m_2) - \left(\frac{M^2}{1+im} + \frac{1}{K} + 2iR\right)},$$
$$a_{27} = \frac{(-a_{18}Gm - a_{10}Gr)}{(m_1+m_2)^2 - (m_1+m_2) - \left(\frac{M^2}{1+im} + \frac{1}{K} + 2iR\right)},$$
$$a_{28} = \frac{(-a_{11}Gr - a_{19}Gm)}{(m_3+m_1)^2 - (m_3+m_1) - \left(\frac{M^2}{1+im} + \frac{1}{K} + 2iR\right)},$$
$$a_{29} = -a_{21} - a_{22} - a_{23} - a_{24} - a_{25} - a_{26} - a_{27} - a_{28}.$$

## References


[1] N. Datta, R.N. Jana, J. Phys. Soc. Jpn. 40 (5) (1976) 1469–1474.
[2] S. Biswal, P.K. Sahoo, Proc. Natl. Acad. Sci. 69A (1994) 46–52.
[3] T. Watanabe, I. Pop, Acta Mech. 108 (1) (1995) 35–47.
[4] E.M. Aboeldahab, E.M.E. Elbarbary, Int. J. Eng. Sci. 39 (2001) 1641–1652.
[5] M. Acharya, G.C. Dash, L.P. Singh, Ind. J. Phys. 75B (1) (2001) 168–176.

[6] B.K. Sharma, A.K. Jha, R.C. Chaudhary, Rom. J. Phys. 52 (5–7) (2007) 487–503.
[7] B. Prabhakar Reddy, J. Anand Rao, J. Eng. Phys. Thermophys. 84 (6) (2011) 1369–1378.
[8] M.C. Raju, S.V.K. Varma, N. Ananad Reddy, Thermal Sci. 15 (2) (2011) 45–48.
[9] U.S. Rajput, Neetu Kanaujia, Int. J. Appl. Sci. Eng. 14 (2) (2016) 115–123.
[10] M. Veera Krishna, B.V. Swarnalathamma, J. Prakash, Applications of Fluid Dynamics XXII (2018) 207–224 Lecture Notes in Mechanical Engineering, doi:10.1007/978-981-10-5329-0_14.
[11] M. Veera Krishna, G. Subba Reddy, A.J. Chamkha, Phys. Fluids 30 (2018) 023106, doi:10.1063/1.5010863.
[12] M. Veera Krishna, A.J. Chamkha, Phys. Fluids 30 (2018) 053101, doi:10.1063/1.5025542.
[13] Reddy N Anand, S.V.K. Varma, M.C. Raju, J. Naval Archit. Mar. Eng. 6 (2009) 84–93.
[14] M. Veera Krishna., M. Gangadhar Reddy, Mater. Today Proc. 5 (2018) 91–98, doi:10.1016/j.matpr.2017.11.058.
[15] M. Veera Krishna., G. Subba Reddy, Mater. Today Proc. 5 (2018) 175–183 https://doi.org/10.1016/j.matpr.2017.11.069.
[16] M. Veera Krishna., Kamboji Jyothi, Mater. Today Proc. 5 (2018) 367–380, doi:10.1016/j.matpr.2017.11.094.
[17] B.S.K Reddy., M. Veera Krishna, K.V.S.N. Rao, R. Bhuvana Vijaya, Mater. Today Proc. 5 (2018) 120–131, doi:10.1016/j.matpr.2017.11.062.
[18] S.M.M.c, M.A. EL-Hakiem, A.M. Rashad, J. Comput. Appl. Math. 213 (2) (2008) 582–603, doi:10.1016/j.cam.2007.02.002.
[19] A.M. Rashad, S. Abbasbandy., Ali J. Chamkha, J. Heat Transf. 136 (2) (2014) 022503, doi:10.1115/1.4025559.
[20] Ali J. Chamkha, A.M. Rashad, Eisa Al-Meshaiei, Int. J. Chem. React. Eng. 9 (2011) A113.
[21] A.Y. Bakier, A.M. Rashad, M.A. Mansour, Commun. Nonlinear Sci. Numer. Simul. 149 (5) (2009) 2160–2170, doi:10.1016/j.cnsns.2008.06.016.
[22] M.J. Lighthill, Philos. Trans. R. Soc. Lond. 252A (1960) 397–430.
[23] G. Sutton, A. Sherman, Engineering Magnetohydrodynamics, Mc Graw Hill, New York, 1965.
[24] M.M. Rashidi, N. Rahimzadeh, M. Ferdows, Md Jashim Uddin, O. Anwar Bég, Chem. Eng. Commun. 199 (8) (2012) 1012–1043.
[25] M.M. Rashidi, M.M. Bhatti, M.A. Abbas, M.E. Ali, Entropy 18 (4) (2016) 117.
[26] M.M. Bhatti, M. Ali Abbas, M.M. Rashidi, Appl. Math. Comput. 316 (1) (2018) 381–389, doi:10.1016/j.amc.2017.08.032.
[27] S. Hamed, M.M. Rashidi, Adv. Powder Technol. 27 (2016) 171–178, doi:10.1016/j.apt.2015.11.014.
[28] M.M. Rashidi, S. Abelman, N. Freidooni Mehr, Int. J. Heat Mass Transf. 62 (2013) 515–525, doi:10.1016/j.ijheatmasstransfer.2013.03.004.
[29] M. Veera Krishna, Ali J. Chamkha, J. Porous Media 22 (2) (2019) 209–223, doi:10.1615/JPorMedia.2018028721.
[30] M. Veera Krishna, K. Bharathi, Ali. J. Chamkha, Interfacial Phenom. Heat Transf. 6 (3) (2019) 253–268, doi:10.1615/InterfacPhenomHeatTransfer.2019030215.
[31] M. Veera Krishna, K. Gangadhara Reddy, A.J. Chamkha, Trends Math. (2019) 417–427, doi:10.1007/978-3-030-01123-9_41.
[32] M. Veera Krishna, M. Gangadhara Reddy, A.J. Chamkha, Int. J. Fluid Mech. Res. 45 (5) (2019) 1–25, doi:10.1615/InterJFluidMechRes.2018025004.
[33] H.P. Greenspan, The Theory of Rotating Fluids, Cambridge University Press, London, 1969.
[34] T.G. Cowling, Magnetohydrodynamics, Interscience Publishers, New York, 1957.